The 2009 IEEE/RSJ International Conference on
Intelligent Robots and Systems
October 11-15, 2009 St. Louis, USA

Analysis and optimization of obstacle clearance of articulated rovers

Faïz Ben Amar, Pierre Jarrault, Philippe Bidaud, Christophe Grand
ISIR - Institut des Systèmes Intelligents et Robotiques
Université Pierre et Marie Curie Paris 6, CNRS UMR 7220
4, place Jussieu - 75252 Paris Cedex 05 - France
{amar,jarrault,bidaud,grand}@isir.upmc.fr

***Abstract*— The paper develops a method for analyzing and improving by control obstacle clearance capacities of articulated multi-wheeled rovers. On uneven ground surface, load and traction force distributions through the wheel/ground contact system are highly coupled. They are both conditioned by the global equilibrium of the mechanical system and the contact stability constraints. The optimal traction force distribution problem is formulated here as a convex optimization problem using Linear Matrix Inequalities (LMIs). Velocity and force transmissions in articulated multi-wheeled mobile robots are introduced under a generic form decomposed in task, joint and contact levels. A tyre-model is used for the evaluation of the robustness of the solution with respect to slippage phenomena. Simulation results show that the traction distribution forces which is so determined lead to a significant increase in obstacle clearance capacities compared to an usual velocity control technique.**

***Index Terms*— Rovers, obstacle clearance, mobility, kinematics**

I. INTRODUCTION

Mobile robotic systems use dedicated elements for propulsion, such are wheels, tracks or legs, which are integrated into a mechanical system. Generally they present internal mobilities allowing an active or passive adaptation to geometrical complexity of the ground and more generally to their operational environment. Locomotion systems can be seen as multi-body articulated systems interacting with the environment by a set of unilateral contacts with adhesion or slippage, the number and the nature of those contacts evolving in time and space. From a topological point of view, locomotion systems can be compared to articulated hands and the analysis of the mechanical properties of locomotion systems can be inspired by grasp analysis. Force and velocity transmissions in these systems can be analyzed by the use of similar mathematical tools, as for the optimization of contact force distribution [1] or for evaluating quantitatively the obstacle clearance capabilities [2].

The work developed in this paper tries to bring an answer to the evaluation of traction capabilities and the optimal traction distribution for obstacle clearance of wheeled-based mobile robots evolving on uneven surfaces. Off-road mobile robots have generally complex structure (several joints for suspension or for auxiliary locomotion modes). Comparatively to cars, suspension mechanism mobilities of mobile robots satisfy to different functionality operational needs: they have to ensure a permanent contact with a highly irregular ground surface, to contribute to robot stabilization and sometimes to its propulsion like in walking locomotion systems for instance [3].

Most of articulated wheeled robots have 6 wheels, which are either multi-platforms or mono-platform. The formers are generally composed by 3 articulated axles called modules [4], and the seconds one have a main body and more complex mechanisms such as rocker-bogie structure [5] [6], or with multi-parallelogram systems [7]. Generally, the motion of these systems are controlled by using their differential kinematic model. The method for deriving the input/output velocity relationship consists in introducing geometrical transformations between the moving bodies and their time-derivative in order to obtain velocity equations by assuming ideal rolling conditions between the wheels and the ground, as closed-loop constraints [8]. Systematic formulations have been developed for various combinations of driving and steering wheels [9] [10]. Sliding models in the wheel/ground interaction have been also introduced for developing more realistic models [11] [12] [3].

The problem of obstacle clearance of off-road robots has been addressed slightly, in particular either from experimental point of view or by using dynamic simulation [13] [6]. However, there is no theoretical study based on analytical formulation of the problem of force and velocity transmissions between joint, contact and task spaces.

The paper proposes a general framework for analysis and optimization of the obstacle clearance process. The framework can be applied to any articulated wheeled system with active or passive mobilities. The method is based on a kineto-static model which takes into account the slippage and friction condition in wheel-ground contacts. In the next section, we first present the kinematics of the considered robot and then we develop its kineto-static model used for the analysis and the optimization. After, we discuss the

mechanical model of the wheel-ground contact and show the similarities between the Coulomb friction model and the tyre model. Section (4) draws up the problem of contact force distribution in multi-wheeled articulated robots and proposes a formulation based on a convex optimization that involves linear matrix inequalities LMIs. The method defines the stability contact by using the maximal friction condition. Simulation results developed in the last section show the efficiency of the method and its robustness in relation to a realistic tyre model that considers wheel slippage. Results are also compared to a simple control method based on an equi-distribution of wheel's rate and demonstrate the relevance of the optimization of force distribution.

Fig. 1. RobuRoc6 negotiating an obstacle.

II. KINETO-STATIC MODEL OF ROBUROC6

The vehicle considered in this paper is called RobuROC6 (figure 1). It can be considered as a series of 3 monocycles modules linked together by two orthogonal revolute joints allowing roll and pitch motions of each module. Each monocycle module is steered and driven by two actuated conventional wheels on which a lateral slippage may occur. The rear and the front modules are symmetrically arranged about the central one. The two revolute joints along the pitch axis are coupled by means of 4 hydraulic actuators with interconnected cylinders. This interconnection ensures that the front and rear pitch joints rotate symmetrically with respect to the middle axle. This kinematics permits to transform RobuRoc6 into a 4-wheel configuration as shown in figure (2) mainly to increase its manoeuvrability when needed. However the robot could operate without actuating the hydraulic pump and then the pitch suspension works as a differential mechanical system.

In this paper, we restrain the analysis to the sagittal plane and we will not consider the parallel mechanisms composed by the hydraulic cylinders controlling the pitch rotoide joints. We consider also that the pitch suspension is not actuated, and that the robot has all its wheels in contact with the ground.

We establish in this section for the considered rover (fig.3) the relationships between the time-derivative of joint

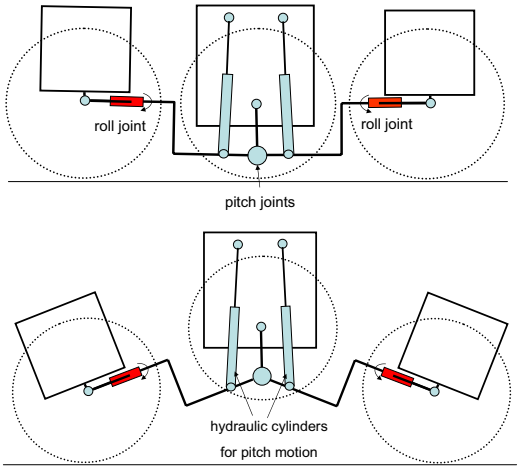

Fig. 2. Kinematics scheme of RobuROC6 : 2 configurations illustrating the central module manipulation.

parameters $\dot{\boldsymbol{\theta}}$ and the middle axle absolute velocity $\dot{\mathbf{x}}$. We study here the 2D sagittal motion of the vehicle, then only one suspension mobility around the pitch axis will be taken into account. The two mobilities of front and rear axle around the roll axis will not be considered in this analysis. Likewise, the closed kinematic loops of hydraulic cylinders actuating the pitch motion (fig.2) are not considered in this model. We denote by ψ the pitch motion parameter of the front axle and then by $-\psi$ for that of the rear one, by $\theta_1, \theta_2, \theta_3$ the joint parameters of respectively the front, the central and the rear wheel. We denote also by $\mathbf{x} = (x, z, o)$ planar position and orientation of the central axle expressed in the wheel center P. Then joint and task parameters are respectively $\boldsymbol{\theta} = (\psi, \theta_1, \theta_2, \theta_3)^{\mathrm{t}}$, $\mathbf{x} = (x, z, o)^{\mathrm{t}}$.

For each wheel-ground contact C_i, thanks to motion composition principle we can write

$$\vec{V}(C_i, S_P/S_0) = -\vec{V}(C_i, S_{W_i}/S_P) + \vec{V}(C, S_{W_i}/S_0) \quad (1)$$

where S_P, S_0, S_{W_i} denote frames attached to the platform (central module), the ground and the ith wheel. $\vec{V}(C_i, S_P/S_0)$ represents, in point C_i, the platform twist with respect to the ground, then it can be expressed by an adjoint matrix in se(2), $\vec{V}(C_i, S_{W_i}/S_P)$ characterizes the velocity of point C_i with respect to the platform, then it can be given by a jacobian matrix, and $\vec{V}(C, S_{W_i}/S_0)$ is a slippage velocity in the wheel-ground contact.

Applying again the motion composition law along the kinematic path joining S_{W_i} to S_P, we obtain respectively for the front, center and rear contacts

$$\begin{aligned}
u\vec{i} + v\vec{k} + \dot{o}\vec{j} \times \vec{a}_1 &= -\dot{\psi}\vec{j} \times \vec{b}_1 - \omega_1\vec{j} \times -r\vec{n}_1 + \vec{v}_{s,1} \\
u\vec{i} + v\vec{k} + \dot{o}\vec{j} \times -r\vec{n}_2 &= -\omega_2\vec{j} \times -r\vec{n}_2 + \vec{v}_{s,2} \\
u\vec{i} + v\vec{k} + \dot{o}\vec{j} \times \vec{a}_3 &= +\dot{\psi}\vec{j} \times \vec{b}_3 - \omega_3\vec{j} \times -r\vec{n}_3 + \vec{v}_{s,3}
\end{aligned}$$

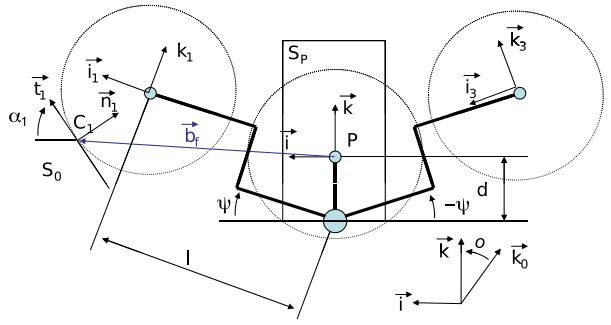

Fig. 3. Planar scheme of the suspension kinematics and geometrical parameters definition.

where $(u, v)^t = \mathbf{R}_o(\dot{x}, \dot{z})^t$ are velocity components of the center of the middle wheel expressed in the local platform frame $(P, \vec{i}, \vec{k})$, $\omega_i = \dot{\theta}_i$ is the rate of the ith wheel, r is wheel radius, $\vec{b_1}, \vec{b_3}$ are vectors from point P to, respectively, the front and rear contact points C_1 and C_3, $\vec{v}_{s,i}$ is the wheel-ground slippage velocity in the ith contact. By projecting these equations along the tangential and normal vectors $\vec{t}_i$ $\vec{n}_i$ of contact frames (figure (3)), we obtain

$$\mathbf{G}^t \begin{pmatrix} \dot{x} \\ \dot{z} \\ \dot{o} \end{pmatrix} = \mathbf{J} \begin{pmatrix} \dot{\psi} \\ \omega_1 \\ \omega_2 \\ \omega_3 \end{pmatrix} + \mathbf{v_s} \tag{2}$$

with

$$\mathbf{G}^t = \begin{pmatrix} C_{\alpha_1} & -S_{\alpha_1} & -r + a_\psi C_{\alpha_1} + b_\psi S_{\alpha_1} \\ S_{\alpha_1} & C_{\alpha_1} & a_\psi S_{\alpha_1} - b_\psi C_{\alpha_1} \\ C_{\alpha_2} & -S_{\alpha_2} & -r \\ S_{\alpha_2} & C_{\alpha_2} & 0 \\ C_{\alpha_3} & -S_{\alpha_3} & -r + a_\psi C_{\alpha_3} - b_\psi S_{\alpha_3} \\ S_{\alpha_3} & C_{\alpha_3} & a_\psi S_{\alpha_3} + b_\psi C_{\alpha_3} \end{pmatrix} \mathbf{R}_o, \tag{3}$$

$$\mathbf{J} = \begin{pmatrix} r - b_\psi S_{\alpha_1} - c_\psi C_{\alpha_1} & r & 0 & 0 \\ b_\psi C_{\alpha_1} - c_\psi S_{\alpha_1} & 0 & 0 & 0 \\ 0 & 0 & r & 0 \\ 0 & 0 & 0 & 0 \\ -r - b_\psi S_{\alpha_3} + c_\psi C_{\alpha_3} & 0 & 0 & r \\ b_\psi C_{\alpha_3} + c_\psi S_{\alpha_3} & 0 & 0 & 0 \end{pmatrix}, \tag{4}$$

$$\begin{cases} a_\psi = dC_\psi - d - lS_\psi \\ b_\psi = lC_\psi + dS_\psi \\ c_\psi = dC_\psi - lS_\psi \end{cases}, \tag{5}$$

$$\mathbf{R}_o = \begin{pmatrix} C_o & -S_o & 0 \\ S_o & C_o & 0 \\ 0 & 0 & 1 \end{pmatrix} \tag{6}$$

where $C_x = \cos x$, $S_x = \sin x$, l and d are constant kinematic parameters defined on figure (3).

The principle of virtual work leads to the dual static model,

$$\begin{cases} \mathbf{Gf} = \mathbf{g_x} \\ \mathbf{J^t f} = -\boldsymbol{\tau} + \mathbf{g}_{\boldsymbol{\theta}} \end{cases} \tag{7}$$

which represents the equilibrium equations of the system subject to generalized gravitational forces $\mathbf{g}$, joint actuator torques $\boldsymbol{\tau}$ and contact forces $\mathbf{f}$. As kinematic contact conditions (2) are given in the local contact frame $(\vec{t}_i, \vec{n}_i)$, the contact force vector is composed with tangential and normal components $\mathbf{f} = (f_{1,T}, f_{1,N}, f_{2,T}, f_{2,N}, f_{3,T}, f_{3,N})^t$.

$\mathbf{g}$ is the generalized force due to gravity. It can be computed by $\mathbf{g_x} = \frac{\partial U}{\partial \mathbf{x}} = \mathbf{w}$, $\mathbf{g}_{\boldsymbol{\theta}} = \frac{\partial U}{\partial \boldsymbol{\theta}}$ with U the total potential energy. We obtain:

$$\mathbf{g_x} = \begin{pmatrix} 0 \\ (m_1 + m_2 + m_3)g \\ -m_1 g(a_\psi S_o + b_\psi C_o) + m_3 g(-a_\psi S_o + b_\psi C_o) \end{pmatrix}$$

$$\mathbf{g}_{\boldsymbol{\theta}} = \begin{pmatrix} -m_1 g(c_\psi S_o + b_\psi C_o) + m_3 g(c_\psi S_o - b_\psi C_o) \\ 0 \\ 0 \\ 0 \end{pmatrix}$$

These generalized forces assume that the center of gravity of each module is located on its axle. m_i depicts the mass of the ith module and g the gravitational acceleration.

III. Wheel-ground contact model

Robot-ground interaction is of high importance in land locomotion. Moreover, wheeled-based locomotion systems have continuous contacts with the ground. An efficient vehicle navigation needs a realistic model that characterizes force and velocity transmission through this contact. In first approximation, the contact can be modeled by an ideal rolling contact without slippage and a Coulomb friction law. This is a first order model which is commonly used for grasping and for locomotion analysis. However, this model could be not sufficient when the friction and the stiffness of the contact are slight. For off-road as well as for on-road vehicles, the contact model expresses the force and moment components as function of the contact geometry, the relative displacement parameters and their time-derivative. Most of tyre models uses for characterizing the longitudinal slippage, the following ratio:

$$\begin{aligned} s_i &= \frac{v_{s,i}}{\sup(r\omega_i, v_i)} \\ &= \frac{v_i - r\omega_i}{\sup(r\omega_i, v_i)} \end{aligned} \tag{8}$$

where v_i is the longitudinal linear velocity of the wheel center. The sup function allows to avoid division by zero in case of pure spinning ($v_i = 0$) or total wheel locking ($\omega_i = 0$).

Equation (2) can be split into two parts, according the normal (N) and tangential (T) projections

$$\begin{cases} \mathbf{G}_N^t \dot{\mathbf{x}} - \mathbf{J}_{N,\psi} \dot{\boldsymbol{\psi}} &= 0 \\ \mathbf{G}_T^t \dot{\mathbf{x}} - \mathbf{J}_{T,\psi} \dot{\boldsymbol{\psi}} - \mathbf{J}_{T,\omega} \boldsymbol{\omega} &= \mathbf{v_s} \end{cases} \tag{9}$$

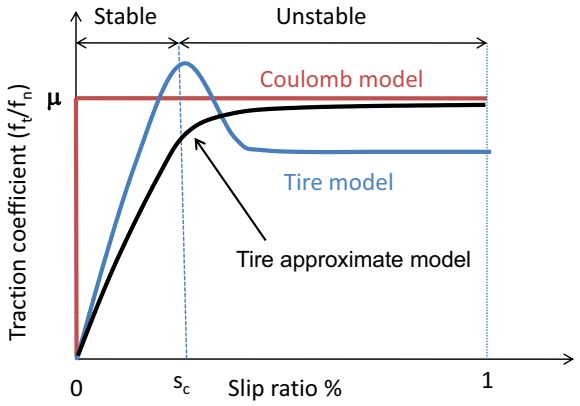

Fig. 4. Tyre traction model and Coulomb friction model.

$\mathbf{J}_{T,\psi}$ and $\mathbf{J}_{T,\omega}$ are jacobians associated to the suspension joint parameter and to wheel's rates. Then the slippage velocity is:

$$\mathbf{v_s} = \left[\mathbf{G}_T^t \mid -\mathbf{J}_{T,\psi}\right] \begin{pmatrix} \dot{\mathbf{x}} \\ \dot{\boldsymbol{\psi}} \end{pmatrix} - \mathbf{J}_{T,\omega}\boldsymbol{\omega} \tag{10}$$

Let $\mathbf{B}_N = \text{null}([\mathbf{G}_N^t \mid -\mathbf{J}_{N\boldsymbol{\psi}}])$, then

$$\begin{pmatrix} \dot{\mathbf{x}} \\ \dot{\boldsymbol{\psi}} \end{pmatrix} = \mathbf{B}_N\boldsymbol{\zeta} \tag{11}$$

Assuming that $\omega_i \neq 0$, the slippage ratio vector can be written:

$$s_i = \frac{\zeta}{r\omega_i}\left(\left[\mathbf{G}_T^t \mid -\mathbf{J}_{T,\psi}\right]\mathbf{B}_N\right)_i - 1 \tag{12}$$

Brush tyre model [14] explains that the contact surface contains two areas: (1) an adhesion area where contact forces are given by the tyre stiffness and the tyre deformation and (2) a slippage area where the elastic forces exceed the friction limit and then contact forces are detrmined only by the friction coefficient and the contact pressure. In this model, when the slippage is above a critical value s_c, all the tyre-ground contact surface is sliding. Below this value, the contact surface has an adhesion area which provides a certain contact stability due to the reversibility of elastic force.

Traction (or braking) force developed by a tire is plotted in general as function of the slippage ratio s_i (figure 4). This curve has a quasi-linear stage whose slope depending on longitudinal tire stiffness and where the contact can be considered stable. The critical slippage value s_c varies from 0.05 to 0.2 depending on tire stiffness, friction coefficient, and contact length. A first-order approximation of a tyre model can be given by the following monotone function:

$$f_{i,T} = \frac{2}{\pi}\mu f_{i,N}\arctan(4s_i/s_c) \tag{13}$$

where μ is the friction coefficient and s_c is a critical slippage which depending on tyre stiffness, contact length...

The next section, considers the optimization problem of traction force distribution and characterizes the friction constraint as expressed by a Coulomb model. The model of tyre is mainly used for simulation of quasi-static motion, for computing stationary slippage ratio and for evaluating the robustness of the optimization in relation to slippage phenomena.

IV. Optimal traction distribution

Traction and load distributions are of great importance when contact geometrical characteristics are uneven i.e. contact normals are not parallel and contact points are not coplanar. In this case, traction and load distribution problems can not be decoupled. We can then use the well known frameworks developed for the analysis of grasping systems. Wheeled mobile systems can be considered as a system where multiple interconnected wheels "grasp" the ground.

If we consider quasi-static equations associated to the generalized parameters (x, z, o) defining the platform and ψ defining the joint suspension parameter, we obtain:

$$\begin{bmatrix} \mathbf{G} \\ -\mathbf{J}_\psi^t \end{bmatrix}\mathbf{f} = \begin{bmatrix} \mathbf{g}_x \\ \mathbf{g}_\psi \end{bmatrix} \tag{14}$$

and can take the compact form

$$\bar{\mathbf{G}}\mathbf{f} = \bar{\mathbf{g}} \tag{15}$$

Solving this model consists in computing $(\mathbf{f})$ for a given configuration $\mathbf{q} = (\mathbf{x}, \boldsymbol{\theta})$ and a given external gravitational generalized force $\mathbf{g}$. Most of models of articulated rovers have a high number of static indeterminacy. This force indeterminacy has two sources : (1) internal, because of the use of a redundant actuation (all the wheels are actuated) and (2) external, because of the multiple frictional wheel/ground contacts. For the considered system, the indeterminacy is equal to 2 when the pitch joint is passive, and is equal to 3 when this joint is actuated.

The main issue of the contact stability problem is to determine a contact force distribution which satisfies :

- unilateral contact condition : $f_{i,N} > 0$,
- no (or small) slippage condition : $(f_{i,T})^2 < (\mu f_{i,N})^2$.

These conditions can be transformed, as proven by [15] and extended by [16], into positive definiteness of certain symmetric matrices which is for a punctual contact with friction (PCWF), restricted here to a planar problem,

$$\mathbf{P(f)} = \sum_{\mathbf{i=1}}^{\mathbf{3}} \mathbf{f_{i,T}S_{i,T}} + \mathbf{f_{i,N}S_{i,N}} > \mathbf{0} \tag{16}$$

with $\mathbf{S}_{i,T}, \mathbf{S}_{i,N}$ are constant block diagonal symmetric matrix. For $i = 1$

$$\mathbf{S}_{1,T} = \text{blockdiag}(\mathbf{E}^2_{12} + \mathbf{E}^2_{21}, \mathbf{0}_{2\times2}, \mathbf{0}_{2\times2})$$

$$\mathbf{S}_{1,N} = \text{blockdiag}(\mu(\mathbf{E}^2_{11} + \mathbf{E}^2_{22}), \mathbf{0}_{2\times2}, \mathbf{0}_{2\times2})$$

and et cetera for $i = 2, 3$. In these relations, $\mathbf{E}^a_{bc}$ is a square matrix of dimension a with element (b, c) to be 1 and all others to be zero.

The problem can be formulated as a set of convex optimization problems involving Linear Matrix Inequalities (LMIs) which can be handled by general-purpose LMI solvers in computationally viable conditions.

We define a measure of optimality for traction forces by

$$\Psi(\mathbf{f}) = w^2 \mathbf{f}^t_T \mathbf{f}_T + \log\det \mathbf{P}^{-1}(\mathbf{f})$$

where $\mathbf{f}_T = (f_{1,T}, f_{2,T}, f_{3,T})^t$ depicts the vector of traction forces, w is a weighting factor. The first term of the measure will grow with the contact tangential forces, and the second term grows to infinity as any contact force approaches the boundary of its friction cone.

The traction force optimization problem can therefore be stated as follows

$$\begin{aligned} &\text{minimize} && \Psi(\mathbf{f}) = \mathbf{f}^t \mathbf{W}^\mathbf{t} \mathbf{W} \mathbf{f} + \log\det \mathbf{P}^{-\mathbf{1}}(\mathbf{f}) \\ &\text{subject to} && \bar{\mathbf{G}}\mathbf{f} = \bar{\mathbf{g}} \end{aligned} \tag{17}$$

with $\mathbf{W}$ corresponds to a weighting matrix of dimensions (6,6) where elements are 0, except $W_{11} = W_{33} = W_{55} = w$.

Finally, wheel torques can be computed by using $\mathbf{J}^t$ and equation (7), which can be written more simply by

$$\tau_i = r F_{i,T} \tag{18}$$

V. Simulation Results

This section gives simulation results of a quasi-static step-like obstacle crossing, using the vehicle and ground parameters given in table (I). The robot crosses a step of height equal to the wheel radius. Geometry of the robot and wheel-ground contacts are computed by integration of velocity parameters and by using the differential kinematic model developed in section (3).

TABLE I

Robot and obstacle parameters.

module mass $m_{1,2,3}$	50Kg
arm length l	0.60m
pitch joint position d	0.10m
wheel radius r	0.25m
Friction coefficient μ	0.8
Step height	0.25m
critical slippage s_c	0.2

Simulations are carried out by Matlab software ™and *cvx* toolbox [17] dealing with convex programming. We compare these results with a simple control model which assumes an

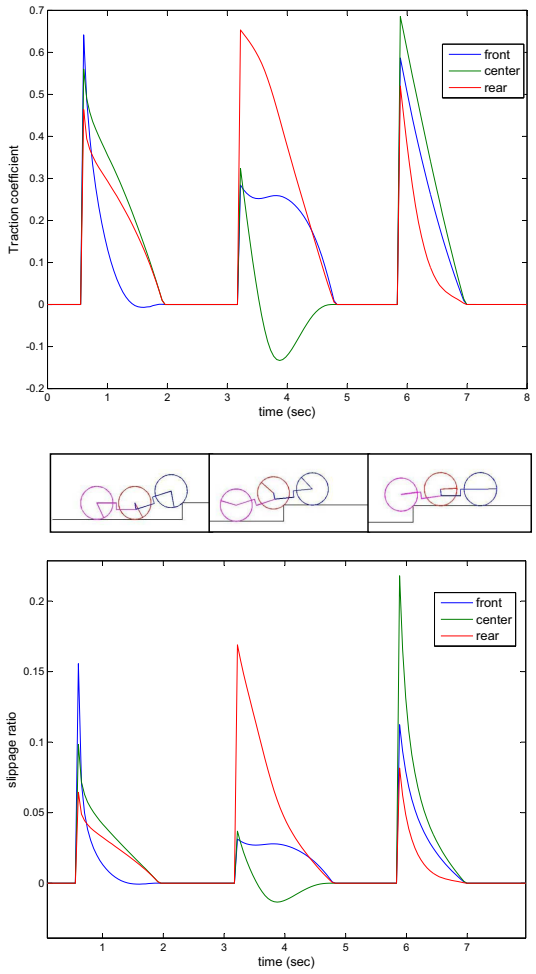

Fig. 5. Traction coefficient f_t/f_n and slippage ratio s_i obtained by traction optimization (weight factor $w = 0.01$).

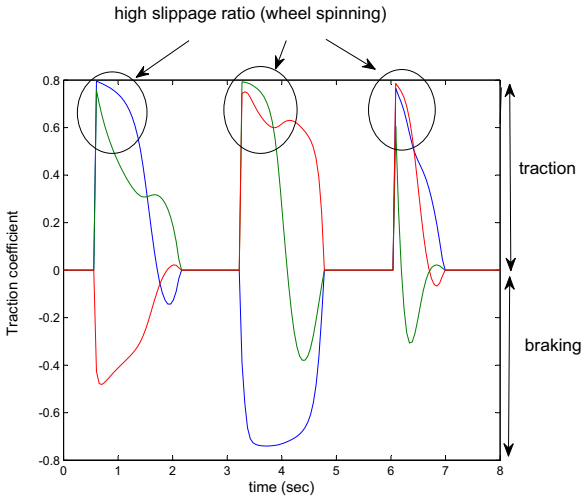

Fig. 6. Traction coefficients with constant velocity distribution.

equal velocity distribution $\omega_i = \omega$. This is a basic control which is usually used as it can be carried out by a simple feedback of the wheel's rate. In this case, we solve the non-linear system equation composed by the 4 equilibrium equations (15) and 4 unknown variables which are the three normal forces $F_{i,N},\ i = 1, 2, 3$ and the slippage parameter $\frac{\zeta}{r\omega}$. Tyre model (13) is used to express tangential forces as function of the last unknown parameters. Curves of figure (6) shows traction coefficients during the step-like obstacle crossing with an equal velocity distribution. The robot can not cross the step as, at each frontal contact two wheels are highly spinning while the other is braking; this latter has a rate smaller than the theoretical ideal rolling rate. We can notice also that high internal forces are created by applying simultaneously tractive and braking torques.

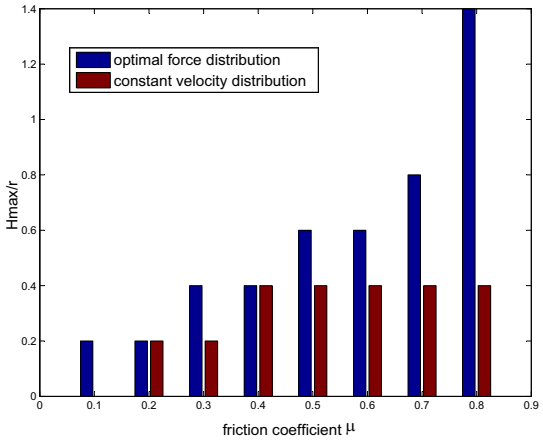

Fig. 7. Maximal obstacle clearance height (divided by the wheel radius) as function of friction coefficient μ, for the two control methods.

More generally, we can show, as seen on the figure (7), that an optimal torque distribution allows high clearance capacity in comparison with a simple velocity control. This plot gives the ratio H_{max}/r for different friction coefficient values μ varying from 0.1 to 0.8, H_{max} is the maximal clearance height of a step-like obstacle.

VI. Conclusion

Taking inspiration from researches in optimal grasping of multifingered tasks, a new method is proposed for computing an optimal traction force distribution in multi-wheeled articulated robot. The method is based on a Linear Matrix Inequalities formulation which leads directly to a simple convex optimization problem that can be solved efficiently in polynomial time. The magnitude of traction forces is used as a measure of optimality of the clearance task. The approach considers cone friction constraint and turns out to be robust to slippage phenomena. This approach has to be extended to 3D motion in order to study for example the effect, of the robot configuration angle along the yaw direction, on the clearance capacity. Experimental validation of such optimal torque distribution requires the estimation of contact parameters (position and normal). However for structured obstacles (stair, step, etc...), this problem can be solved easily by using a ground elevation map and an on-line obstacle sensing.

References

[1] Y. P. Li, T. Zielinska, M. H. A. Jr., and W. Lin, "Vehicle dynamics of redundant mobile robots with powered caster wheels," in *Proc. of the 16th CISM IFToMM Symposium, Romansy*, 2006.

[2] F. Le Menn, P. Bidaud, and F. Ben Amar, "Generic differential kinematic modeling of articulated multi-monocycle mobile robots," *2006. ICRA 2006. Proceedings 2006 IEEE International Conference on Robotics and Automation*, pp. 1505–1510, May 2006.

[3] C. Grand, F. Ben Amar, F. Plumet, and P. Bidaud, "Stability and traction optimization of a reconfigurable wheel-legged robot." *Int. Journal of Robotic Research*, vol. 23, no. 10-11, pp. 1041–1058, 2004.

[4] S. Sreenivasan and K. Waldron, "Displacement analysis of an actively articulated wheeled vehicule configuration with extensions to motion planning on uneven terrain," *Transactions of the ASME*, vol. 118, no. 6, pp. 312–317, 1996.

[5] R. Volpe, "Rocky 7: A next generation mars rover prototype," *Journal of Advanced Robotics*, vol. 11, no. 4, pp. 341–358, 1997.

[6] T. Thueer, A. Ambroise Krebs, R. Siegwart, and P. Lamon, "Performance comparison of rough-terrain robots simulation and hardware," *J. of Field Robotics*, vol. 24, no. 3, pp. 251–271, 2007.

[7] R. Siegwart, P.Lamon, T. Estier, M. Lauria, and R. Piguet, "Innovative design for wheeled locomotion in rough terrain," *Robotics and Autonomous Systems*, vol. 40, pp. 151–162, 2002.

[8] P. Muir and C. Neuman, "Kinematic modeling of wheeled mobile robots," *Journal of robotics systems*, vol. 4, no. 2, pp. 281–340, 1987.

[9] R. Rajagopalan, "A generic kinematic formulation for wheeled mobile robots," *Journal of Robotic Systems*, pp. 77–91, 14-2 1997.

[10] B. Y. Yi and W. Kim, "The kinematics for redundantly actuated omnidirectional mobile robots," *Journal of Robotic Systems*, pp. 255–267, 14-2 2002.

[11] G. M. M. Tarokh, "Kinematics modeling and analyses of articulated rovers," *IEEE Transactions on Robotics and Automation*, vol. 21, no. 4, pp. 539–553, 2007.

[12] K. Iagnemma and S. Dubowsky, "Vehicle wheel/ground contact angle estimation : with application to mobile robot control," in *Proceedings of International Symposium on Advances on Robot Kinematics ARK'00*, 2000, pp. 137–146.

[13] B. C. Bouzgarrou, F. Chapelle, and J. C. Fauroux, "A new principle for climbing wheeled robots: Serpentine climbing with the open WHEEL platform," in *2006 IEEE/RSJ International Conference on Intelligent Robots and Systems,*, Beijing, Oct. 2006, pp. 3405–3410.

[14] H. B. Pacejka, *Tyre and vehicle dynamics*. Oxford, UK: Butterworth–Heinemann, 2002.

[15] M. Buss, H. Hashimoto, and J. Moore, "Dextrous hand grasping force optimization," *IEEE Transactions on Robotics and Automation*, vol. 12, pp. 406–418, 1996.

[16] L. Han, J. C. Trinkle, and Z. Li, "Grasp analysis as linear matrix inequality problems," *IEEE Transactions on Robotics and Automation*, vol. 16, pp. 1261–1268, 2000.

[17] M. Grant and S. Boyd, "Cvx: Matlab software for disciplined convex programming," in *www.stanford.edu/ boyd/cvx/*, ..